THE
PHYSICAL REVIEW

A journal of experimental and theoretical physics established by E. L. Nichols in 1893

SECOND SERIES, VOL. 179, NO. 2 10 MARCH 1969

Relaxation in a Jahn-Teller System. I. Copper in Octahedral Water Coordination

D. P. BREEN,* D. C. KRUPKA,† AND F. I. B. WILLIAMS†
Clarendon Laboratory, Oxford, England
(Received 30 September 1968)

A study has been made, using EPR and electron-spin-echo methods, on the Jahn-Teller systems $La_2Mg_3(NO_3)_{12}\cdot 24H_2O$ and its deuterated counterpart and $Zn(BrO_3)_2\cdot 6H_2O$, all containing substitutional divalent copper. At low temperatures, it is found that the $Cu^{2+}\cdot 6H_2O$ complex exists as a tetragonally distorted octahedron. Anisotropies in the g tensor or random strains may stabilize a distortion. Phonon-induced reorientation of the distortions is observed, using electron-spin-echo methods, and is found to yield a rate τ^{-1} linearly dependent on temperature with a proportionality factor of 5×10^4 deg^{-1} sec^{-1} for $La_2Mg_3(NO_3)_{12}\cdot 24D_2O$ at temperatures up to 12°K. The spin-lattice relaxation rate T_1^{-1} has been measured using the pulse-saturation method and is given by $T_1^{-1}\approx 100T+3.3\times10^{-2}T^5$ for $1.3°K<T<20°K$. Such a low-temperature rate is some four orders of magnitude faster than that observed for Cu^{2+} in the static octahedral water coordination of the KZn Tutton salt. Over the range that both have been measured, $T_1^{-1}\propto\tau^{-1}$.

1. INTRODUCTION

DIVALENT copper in an octahedral environment is one of the best-known examples of the theorem of Jahn and Teller[1] which states that, when an ion is at a site of symmetry sufficiently high that a degenerate state would result for a rigid environment, the actual (elastic) environment spontaneously distorts to lift that degeneracy and lower the over-all energy of the ion plus environment. The first unambiguous experimental evidence for the Jahn-Teller effect was discovered by Bleaney and Bowers[2] in the electron paramagnetic resonance (EPR) spectrum of Cu^{2+} in $ZnSiF_6\cdot 6H_2O$. Similar effects were reported a little later for Cu^{2+} in $La_2Mg_3(NO_3)_{12}\cdot 24H_2O$ [3] and for Cu^{2+} in $Zn(BrO_3)_2\cdot 6H_2O$.[4] (These two hosts will also be called "double nitrate" and "bromate," respectively.) In all three of these materials, the copper ion is surrounded by an octahedron of water molecules. It is in these last two systems that we have studied the relaxation behavior in the hope of further aiding the efforts to interpret theoretically the behavior of these substances.[5–13]

We have divided the work into two papers. Paper I deals primarily with the experimental methods and results and Paper II (henceforth referred to as II) with their interpretation in terms of a model.

The free copper ion has a $3d^9\ ^2D$ ground-state configuration which is split, when placed in an octahedral cubic field, into $^2T_{2g}$ and ^2E_g, as shown in Fig. 1(a). The twofold degenerate ground ^2E state is further split by a field of E-type symmetry produced by an e-mode distortion of the complex [basis (Q_θ,Q_ϵ) shown in Fig. 1(b)]. The first-order electron-ligand coupling predicts a splitting of the electronic degeneracy linear in the distortion amplitude, but the "elastic" energy of the complex increases quadratically [Figs. 1(c) and

* Present address: College St. Albert, Leuven, Belgium.
† Present address: D.Ph.-S.R.M., C.E.N.—Saclay, 91, Gif-sur-Yvette, France.

[1] H. A. Jahn and E. Teller, Proc. Roy. Soc. (London) **A161**, 220 (1937).
[2] B. Bleaney and K. D. Bowers, Proc. Phys. Soc. (London) **A65**, 667 (1952).
[3] D. Bijl and A. C. Rose Innes, Proc. Phys. Soc. (London) **A66**, 956 (1953).
[4] B. Bleaney, K. D. Bowers, and R. S. Trenam, Proc. Roy. Soc. (London) **A228**, 157 (1955).
[5] J. H. Van Vleck, J. Chem. Phys. **7**, 72 (1939).
[6] A. Abragam and M. H. L. Pryce, Proc. Phys. Soc. (London) **A63**, 409 (1950); Proc. Roy. Soc. (London) **A205**, 135 (1951).
[7] W. Moffit and W. Thorson, Phys. Rev. **108**, 1251 (1957).
[8] U. Öpik and M. H. L. Pryce, Proc. Roy. Soc. (London) **A238**, 425 (1957).
[9] H. C. Longuet-Higgins, U. Öpik, M. H. L. Pryce, and R. A. Sack, Proc. Roy. Soc. (London) **A244**, 1 (1958).
[10] I. B. Bersuker and B. G. Vekhter, Fiz. Tverd. Tela **7**, 1231 (1965) [English transl.: Soviet Phys.—Solid State **7**, 986 (1965)].
[11] M. C. M. O'Brien, Proc. Roy. Soc. (London) **A281**, 323 (1964).
[12] F. S. Ham, Phys. Rev. **166**, 307 (1968).
[13] M. D. Sturge, in *Solid State Physics*, edited by F. Seitz and D. Turnbull (Academic Press Inc., New York, 1968), Vol. 20.

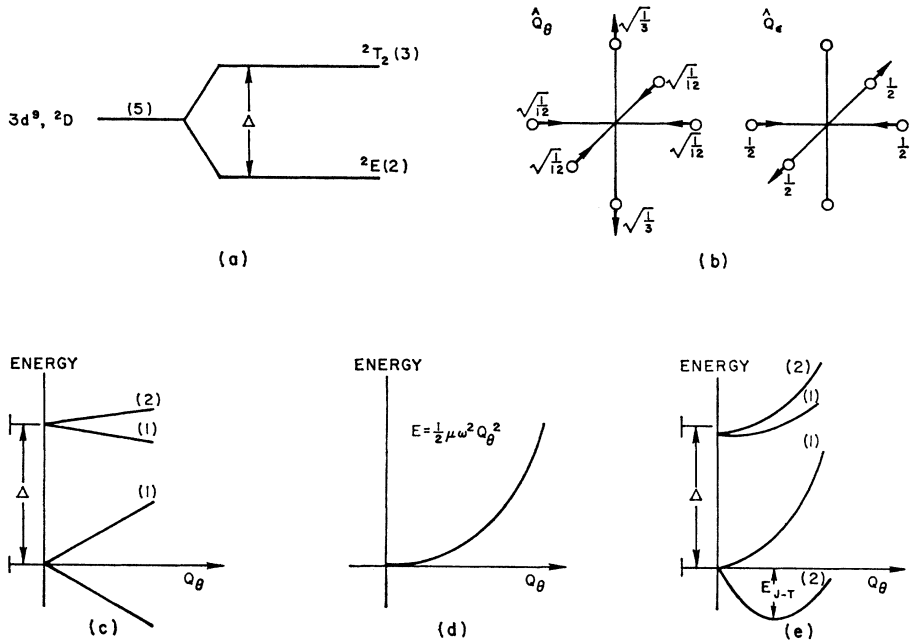

FIG. 1. (a) Behavior of Cu^{2+} energy levels when placed in a rigid octahedral complex. (b) The basis vectors for an E-type distortion. (c) Behavior of Cu^{2+} energy levels when placed in an elastic octahedral complex distorted by stretching along its z axis. (d) The elastic potential versus Q_θ. (e) The total potential ("elastic" and "electronic") versus Q_θ.

1(d)]. The total energy gives the well-known Mexican-hat potential surfaces of Fig. 2(a) of which Fig. 1(e) is a $Q_\epsilon=0$ section. When the zero-point energy $\hbar\omega$ of the e vibrations is small compared with the depth of the potential minimum E_{JT} [see Fig. 2(a)], the Jahn-Teller effect is said to be "static" and the Born-Oppenheimer approximation is quite good, enabling one to calculate the ground-state behavior from the lower potential sheet alone. To put the situation into perspective, representative parameters are expected to be $\hbar\omega\sim300$ cm^{-1} and $E_{JT}\sim3000$ cm^{-1}.[8] The motion on the lower sheet can be divided onto radial and circular components. The radial solutions are harmonic-oscillator-like with quantum energy $\hbar\omega$. The circular motion is due to KE only and the angular momentum around the trough is a constant of the motion. The energies of the vibronic states are then, for the lowest radial state,

$$E=-E_{JT}+\hbar\omega+(\hbar^2/2I)j^2, \qquad (1)$$

where $j=\pm\frac{1}{2}, \pm\frac{3}{2}$, etc., and $I=\mu\rho_0^2$, $\hbar^2/2I\sim10$ cm^{-1}, μ being the effective mass of the e vibration and ρ_0 the distortion amplitude at the potential minimum. Inclusion of the second-order electron-ligand coupling and/or the anharmonic elastic forces warp the potential surface to reduce it from axial to C_{3v} symmetry on the Q_θ-Q_ϵ plot, the minima corresponding to the octahedron pulled along each of its three principal axes.[4] The depth of the wells, 2β, is expected to be about 100–500 cm^{-1}. Because $\beta\gg\hbar^2/2I$, the rotational structure will be considerably modified; it then becomes a good starting point for the lowest three states to talk about (angular) harmonic-oscillator functions localized in each of the three wells. This will be referred to as the $|G_x\rangle$, $|G_y\rangle$, $|G_z\rangle$ representation corresponding to the complex being elongated along each of its principal axes. In such a representation, the diagonal elements in the absence of external perturbations are identical. The states are coupled by the "tunneling" matrix element $\Gamma\sim\beta\gamma$,

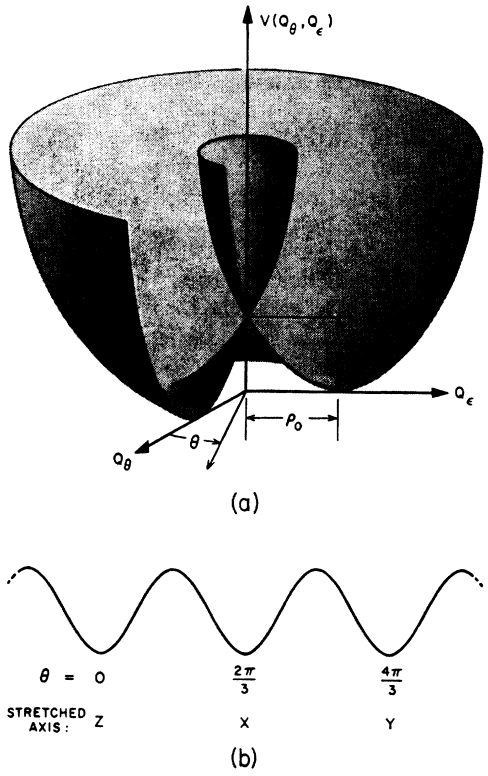

FIG. 2. (a) The Mexican-hat potential for linear coupling. The vectors $\theta=0$, $\theta=\frac{2}{3}\pi$, and $\theta=\frac{4}{3}\pi$ correspond to configurations of the octahedron stretched along its z, x, and y axes, respectively. (b) Section through trough at $\rho=\rho_0$ folded flat, showing the effects of nonlinearities in coupling and of "elastic" anharmonicity.

where γ is the vibrational overlap. For our situation it will be shown in II that $\Gamma \lesssim \frac{1}{10}$ cm^{-1} so that any perturbation—like random strains—which differentiates one well from the other by an amount $\gg\Gamma$ will "stabilize" the system into separate wells. The interpretation of the low-temperature spectrum[4] is that the three lines seen correspond to EPR within each of the three wells, i.e., the resonance spectrum has the appearance of a tetragonally distorted octahedron, with any of the three tetragonal distortions being equally likely. Two possibilities are invoked to explain the single line at high temperature: Either the relaxation from well to well (rate $1/\tau$) becomes so rapid that the three resonance lines are motionally narrowed into one or an excited singlet state, which shows an isotropic resonance line, is populated.

We have studied the interwell relaxation time τ by a spin-echo method and the spin relaxation time T_1 by a pulse-saturation method. We find that up to about 10°K both $1/T_1$ and $1/\tau$ depend linearly on temperature and that T_1 is some four orders of magnitude faster than the similar, but lower-symmetry, non-Jahn-Teller case of Cu^{2+} in the KZn Tutton salt measured by Gill.[14] More significant is that $T_1 \sim 400\tau$, and we show in II how these are related by the model in addition to estimating a value for the tunneling parameter Γ from the magnitude of τ. Above 10°K, $1/T_1$ seems to be described by a T^5 temperature dependence; this behavior, too, is discussed in terms of the model in II.

The apparatus used is described in Sec. 2, while Sec. 3 contains details of the experimental procedure and the results on the angular variation of the spectrum, the interwell reorientation time, and the spin-lattice relaxation time. The discussion follows in Sec. 4. Section 5 forms a summary of the results and serves as a prelude to II.

2. APPARATUS

The apparatus was basically a standard superheterodyne reflection spectrometer operating at 9.4 GHz with provision for injecting pulses of microwaves from a high-power klystron (English Electric K350), as shown in the block diagram of Fig. 3. The TE_{101}-mode sample cavity was provided with the sort of variable coupling arrangement suggested by Gordon[15] and with a dielectric tuning rod necessitated by the fixed frequency of the high-power klystron.

The cavity and the last 10 cm of the waveguide were enclosed in an evacuable space. Temperatures below 4.2°K were obtained by using exchange gas in this space to equilibrate the cavity with the bath whose vapor pressure was controlled by a pump and manostat. For temperatures above 4.2°K, the space was evacuated and the power input to a heater wrapped around the cavity was balanced against the heat leak to the bath through the waveguide. Control to ±0.01°K could be achieved with the help of a carbon resistor in one arm of an ac bridge with a phase-sensitive detector which formed the essential part of a feedback circuit to the heater. Temperatures were measured by He vapor pressure below 4.2°K and by a carbon resistance calibrated against a manganin resistance above that. All temperature readings are judged to be accurate to ±0.1°K.

The monitoring klystron frequency could be phase-locked to the cavity frequency by comparing the phase of the reflected power with that of the incident power, using the 30-MHz phase-sensitive detector and feeding the correction signal onto the klystron reflector. The EPR absorption signal could be observed either directly at the video output of the main amplifier or by a phase-sensitive detector whose reference phase was in quadrature to that used in phase-locking the cavity. The latter scheme has the advantage of being insensitive to the matching condition between the cavity and waveguide, and insures that the detector diodes always operate in the same region determined by the size of the phase reference signal much greater than the absorption signal. With video detection, the sign of the signal for an absorption changes as one swings from under- to overcoupling since the phase reference for the video diode is derived from the reflected signal; when this becomes zero at perfect match there is phase instability. If the signal is comparable with the noise, the noise tends randomly to reverse the signal phase, thus making the detection very nonlinear. Considerable care was taken to insure linearity of detection at all stages to guard against any instrumental modification of recovery shapes.

The high-power klystron was controlled by a direct coupled pulse network. The output pulse shapes had rise and fall times of ~100 nsec, although all the control pulses up to the modulator stage had rise and fall times of ~15 nsec. The high voltage pulse of ~1.7 kV applied to the klystron had rise and fall times of ~75 nsec. The direct coupling insured minimum pulse drop and arbitrary pulse duration for saturation. For relaxation studies the klystron was operated in its recommended mode to give 1–2 W, but for the spin-echo work it was usually run in the next higher mode to give 2–4 W, resulting in some 2 G at the sample.

The pulse-generating network allowed for up to three independently variable klystron command pulses with one fixed and one linearly swept time delay. Suitably synchronized pulses were provided for one or two independently gated boxcar integrators; in the two-pulse spin-echo sequence, the pulse delay could be linearly swept and the boxcar gate signal was swept at double rate to keep pace with the echo. This was done by a circuit which charged a condenser with a constant current for the time t_s of the pulse separation and then discharged it at the same rate until a trigger circuit sensed when it had regained its initial voltage. The linearly swept delay was provided by a circuit which

[14] J. C. Gill, Proc. Phys. Soc. (London) 85, 119 (1965).
[15] J. P. Gordon, Rev. Sci. Instr. 32, 658 (1961).

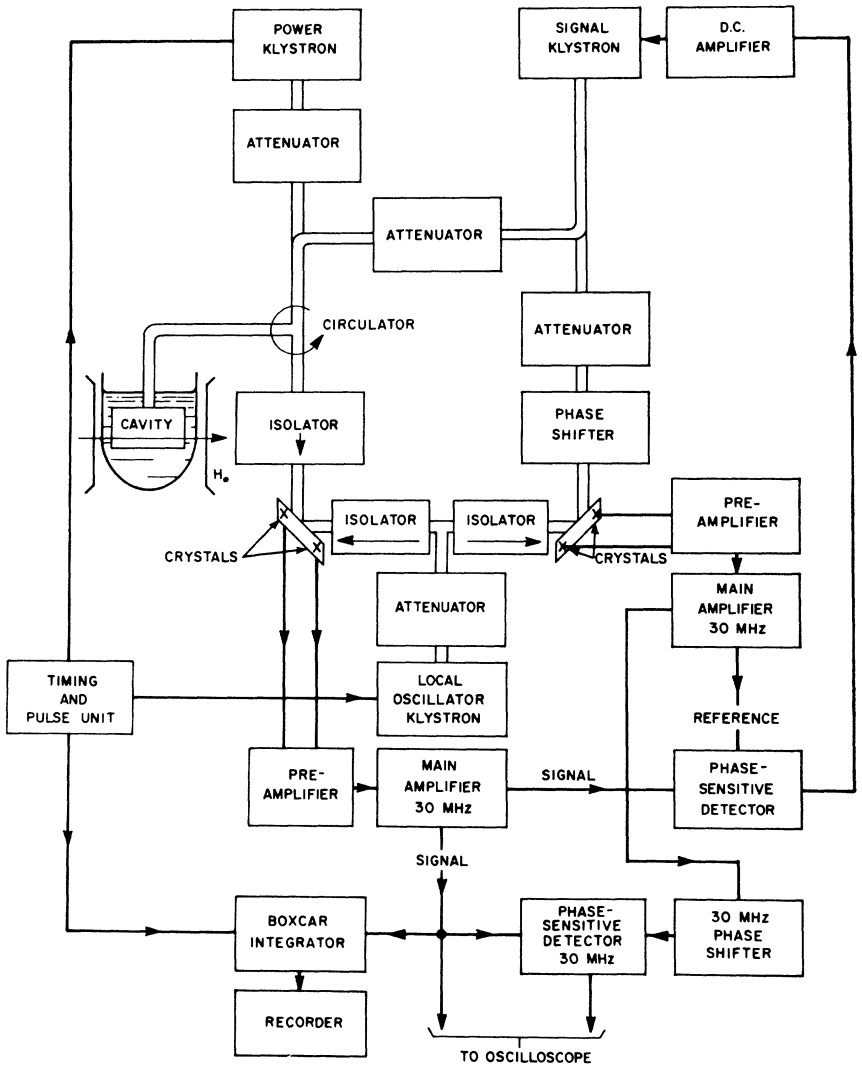

FIG. 3. Block diagram of apparatus.

triggered when a ramp, begun at the initiating pulse, reached a slowly varying datum. By means of these two circuits and a boxcar integrator, we were able to record the spin-echo data directly on a chart recorder rather than having to photograph an oscilloscope trace or make a point-by-point plot. Figure 4 illustrates the pulse network and the timing sequence for a two-pulse spin-echo measurement (τ measurement). The delay t_D was added to allow for the fact that the klystron actually turns on at a time t' later than the command pulses.

The boxcar integrators were just semiconductor diode ring circuits fed by constant current sources—simply Kirchoff's-law devices. The diodes used (Texas Instrument IS-44) were both fast and of sufficiently high backward resistance that output time constants of up to several seconds were feasible. Resolution time of the boxcars was $\sim$100 nsec, linearity $\sim$2% at 1-sec time constant, and maximum gate times $\sim$100 μsec.

Receiver protection was afforded by two devices; the input of the 30-MHz preamplifier was shorted by two very fast Ge diodes connected back to back to prevent large transients in the input circuit and the local-oscillator klystron was frequency shifted by a blanking pulse applied to its reflector so that the i.f. during a power pulse fell outside the bandwidth of the amplifiers. The Ge diodes did not affect the linearity for small signals, but did prevent large transients building up which would have rung too long before falling to the low signal level. The local-oscillator blanking was not necessary with spin-echo-length pulses of less than 1 μsec, but was necessary with the long pulses required for saturation, presumably because over the longer period the amplifier power supplies were overrun.

Spin-lattice relaxation rates were usually measured by photographing an oscilloscope presentation of the absorption signal recovery using the phase-sensitive detection scheme outlined earlier. Some measurements

were made by sampling the z magnetization with a two-pulse spin-echo sequence[16] a swept delay time after the end of the saturating pulse, and recording that on a chart recorder via a boxcar integrator. A two-boxcar scheme with cw monitoring was also tried and found to work quite well: One boxcar was set at a fixed position well into the tail of the recovery to sample the "base line" while another was swept slowly over the recovery. The outputs were subtracted to eliminate low-frequency noise at $\omega \ll 1/T_1$ and presented on a chart recorder. This scheme was not pursued, but it did give a signal-to-noise ratio superior to that obtained by the photographic method.

3. EXPERIMENTAL

Sample Preparation

The $La_2Mg_3(NO_3)_{12}\cdot 24H_2O:Cu^{2+}$ crystals were prepared from both Johnson-Matthey spectrographically standardized and 99.997% pure Lindsay Chemical Co. materials with special care taken to avoid contamination during growth. The crystals were grown by evaporation from a thermally stabilized water solution at Oxford room temperature or 0°C; deuteration was accomplished by redissolving in heavy water four times. The impurity concentration was checked for one sample mass spectrographically; the only paramagnetic impurity found was 1.5 ppm by weight (3.3×10^{16} cm^{-3}) of Fe. As a further indication that results were not affected by impurities, the relaxation time of $\frac{1}{2}$ at.% of Nd^{3+} was checked to be $\sim\frac{1}{2}$ sec at 1.3°K in agreement with Scott and Jeffries.[17] As reported by Bleaney, Bowers, and Trenam[4] the Cu^{2+} concentration in the crystals was considerably less than that in the parent solution when this was in large excess; the final crystals were withdrawn while there was still an abundance of mother solution to avoid excessive Cu inhomogeneity. Copper concentrations were determined spectrochemically for most samples subsequent to the resonance measurements. In addition to the samples grown by us, one crystal was obtained from J. W. Leight of the Carlyle Barton Laboratory of Johns Hopkins University.

A more limited set of measurements was made for $Zn(BrO_3)_2\cdot 6H_2O:Cu^{2+}$. These crystals were prepared from chemicals whose purity was not guaranteed by the manufacturer, but at least no spin resonance was detected in undoped samples. A mass spectrographic analysis showed the only paramagnetic impurity to be 1.3×10^{17} cm^{-3} of Fe. The Cu-doping level was again determined spectrochemically.

The Spectrum and Spin Hamiltonian

Procedure

Accurate determination of the spin-Hamiltonian parameters for the double nitrate was made possible through the use of an externally rotatable platform inside a TE_{101} cavity, the axis of rotation of the platform being perpendicular to the rotation axis of the magnet. The cavity and the X-band spectrometer used for this purpose were made available by Dr. E. R. Davies of the Clarendon Laboratory. Measurements were made at 20°K on a deuterated sample grown from a solution having a 4% Cu^{2+} concentration. A spot check at 4.2°K for the spectrum at one easily reproducible direction revealed identically the same spectrum as obtained at 20°K.

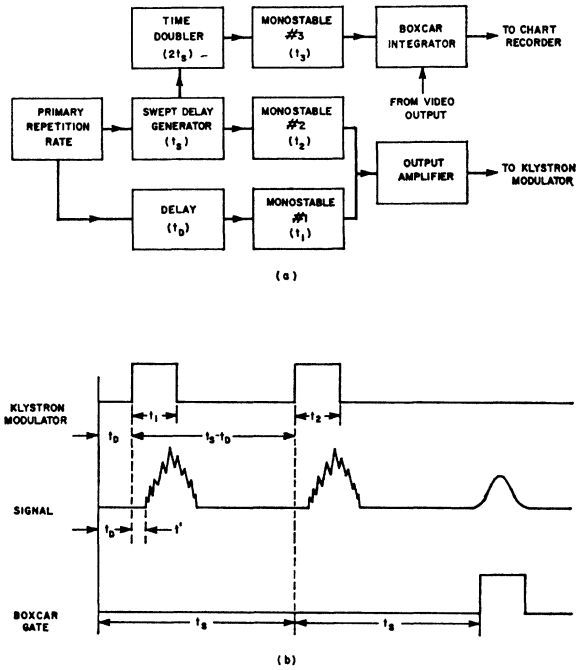

FIG. 4. (a) Pulse network arranged for two-pulse spin echoes. (b) Pulse-timing sequence derived from (a).

The platform and magnet were first positioned so that the three spectra coincided.[4] The magnet was then rotated and the spectra recorded at regular intervals until one obtained the largest g value without rotating the previously adjusted platform. At this point, the platform was rotated to check whether in fact this position yielded a maximum g value. Next, similar operations were carried out to obtain the field orientation yielding the minimum g value. The parameters obtained in this experiment were determined from a run in which no rotation of the platform was required beyond the initial adjustment required to bring the spectra into coincidence.

On the assumption that the principal axes of the g tensor are indeed along the x, y, and z distortions of the water octahedron,[4] the operations described above correspond to rotating the magnetic field in the $(1\bar{1}0)$ plane from the [111] to the [001] direction, and then to the [110] direction. Special precautions were taken in examining the spectra near the [111] direction; here they were recorded every 0.25°.

[16] A. Kiel and W. B. Mims, Phys. Rev. **161**, 386 (1967).
[17] P. L. Scott and C. D. Jeffries, Phys. Rev. **127**, 32 (1962).

Results

Deuterated double nitrate. Although there are two possible substitutional sites for Cu^{2+} in $La_2Mg_3(NO_3)_{12}\cdot 24H_2O$,[18] the spectrum of only one site was observed; this matter is discussed in II. For the site observed, the direction yielding the largest g value is at $55.4°\pm0.5°$ from the direction at which the three spectra coincide, while that yielding the minimum g is at $34.9°\pm0.5°$ from the latter direction. Thus, within the accuracy possible in our experiments, the spectra observed correspond to distortions along the x, y, and z distortions of the octahedron. The spectra of each distorted site may be described by an axial spin Hamiltonian. For a complex elongated along the z direction, this is

$$\begin{aligned}\mathcal{H}=&g_{\parallel}\beta H_zS_z+g_{\perp}\beta(H_xS_x+H_yS_y)\\&+A_{\parallel}S_zI_z+A_{\perp}(S_xI_x+S_yI_y)\\&+P_{\parallel}[I_z^2-\tfrac{1}{3}I(I+1)]-\gamma\beta_N\mathbf{H}\cdot\mathbf{I},\end{aligned}\quad(2)$$

where

$$\begin{aligned}g_{\parallel}&=2.465\pm0.001,\\ g_{\perp}&=2.099\pm0.001,\\ A_{\parallel}&=(-111.7\pm0.5)\times10^{-4}\ \text{cm}^{-1},\\ A_{\perp}&=(16.0\pm0.5)\times10^{-4}\ \text{cm}^{-1},\\ P_{\parallel}&=(10.5\pm0.5)\times10^{-4}\ \text{cm}^{-1}.\end{aligned}$$

The values for $A_{\parallel}$, $A_{\perp}$, and $P_{\parallel}$ are means weighted in proportion to the natural abundances of the isotopes Cu^{63} and Cu^{65}.

Spin-Echo Measurements

Procedure

In the two-pulse measurements, two 90° pulses of approximately 0.5-μsec duration and producing a field H_1 (in the rotating frame) of about 1 G were applied at $t=0$ and $t=t_s$. The separation between the pulses was swept electronically as described above and the echo amplitude was monitored using a boxcar amplifier with a gatewidth of about 1 μsec and a time constant of 1 sec. Since some of the pulse power was reflected from the cavity into the detecting system, a dead time of approximately 2 μsec resulted.

Some "stimulated-echo" experiments were also done. In this case a pair of 90° pulses at fixed separation t_s was applied and followed by a third pulse at time $t=T+t_s$. The stimulated echo, occurring at $t=T+2t_s$, was again electronically tracked with the boxcar amplifier.

Decay of Spin-Echo Signal

The formation and decay of electron spin echoes is described by Mims, Nassau, and McGee (MNM)[19] and by Klauder and Anderson.[20] The reader is referred to them for an introduction to this subject. These earlier studies were concerned with spectral diffusion in inhomogeneously broadened lines, the idea being similar to burning holes and monitoring the rate at which these are filled in. The mechanism studied by MNM is the spread of excitation *within* a dipolar broadened spin packet, and, for such a case, they find that the decay factor for the envelope of the two-pulse spin-echo signal is given by $\exp(-mt_s^2)$, characteristic of Lorentzian diffusion. Here m is a factor depending on the mechanisms giving rise to the diffusion. Gaussian diffusion leads to a decay factor given by $\exp(-kt_s^3)$, where k once again depends on the diffusion mechanisms.

In this study we are concerned primarily with an entirely different process for echo decay. At each Cu^{2+} site one expects some anisotropy such as random strains to stabilize a certain distortion of the water octahedron. The complex will spend more of its time in this stabilized distortion, occasionally jumping to another distortion and returning. Consider now, for example, an experiment in which one has oriented and adjusted the static magnetic field such as to obtain a signal from those spins belonging to sites with some effective g, say, g_1. If at any time following the first pulse a complex with a spin contributing to the resonant precessing magnetization jumps to another distortion with an effective g different from g_1, a possible contribution to the signal is lost. Since the jumps occur independently, the resulting decay factor for the envelope will be $\exp(-2t_s/\tau)$, where $1/\tau$ is the rate at which the complex jumps from one distortion to another. The following points are to be noted. A spin jumping from the resonant distortion and returning to it will not contribute to the echo because it will have accumulated a random phase difference $(g_1-g_2)\beta Ht/\hbar$ while precessing in a field H for a time t in a distortion with an effective g_2. Similarly, the spins scattered into the resonant distortion do not contribute since they arrive with random phase. This mechanism for loss of phase memory is obviously inoperative when $(g_1-g_2)\beta Ht/\hbar\ll1$, e.g., when the magnetic field is so oriented as to yield $g_1=g_2$. In the experiments described here it will be seen that there is a self-consistency check on the time t, indicating that it is sufficiently long.

Results

Double nitrate. The results to be described were obtained on strong lines in the "perpendicular spectrum." It was found that these showed the least pronounced modulation[19,21,22] due to the precession of the neighboring nuclei. A smooth curve was drawn through the decay trace, and the background, determined by repeat-

[18] A. Zalkin, J. D. Forrester, and D. H. Templeton, J. Chem. Phys. **39**, 2881 (1963).
[19] W. B. Mims, K. Nassau, and J. D. McGee, Phys. Rev. **123**, 2059 (1961).
[20] J. R. Klauder and P. W. Anderson, Phys. Rev. **125**, 912 (1962).
[21] L. G. Rowan, E. L. Hahn, and W. B. Mims, Phys. Rev. **137**, A61 (1965).
[22] D. Grischkowsky and S. R. Hartmann, Phys. Rev. Letters **20**, 41 (1968).

ing the steps required to obtain the decay trace but moving H_0 well off resonance, was subtracted, and the result plotted on semilog paper (see Fig. 5). Such a procedure was repeated for temperatures ranging from 1.3 to ~12°K. The plots for a number of crystals are shown in Fig. 6 and the salient results are summarized in Table I. The results for two samples obtained by photographing the decay on an oscilloscope are also included.

Bromate. In addition to the data on Cu^{2+} in LMN some measurements were also made on Cu^{2+} in $Zn(BrO_3)_2 \cdot 6D_2O$. This system indicated a phase memory time of about 1.5 μsec at 4.2°K. The data were not reproducible, however; it is believed that measurement of such a short phase memory time was really beyond the capability of our apparatus.

We also attempted unsuccessfully to observe spin echoes for Ni^{3+} in Al_2O_3. The sample used in this case was cut from the same boule as used in the acoustic-loss measurements of Sturge *et al.*[23]

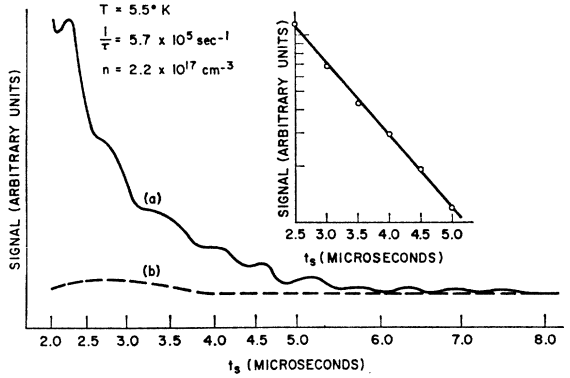

FIG. 5. Boxcar integrator recording of (a) echo-decay trace and (b) the background obtained by tuning H_0 well of resonance. Inset shows the results obtained by drawing a smooth line through (a), subtracting (b), and plotting the result on semilog paper.

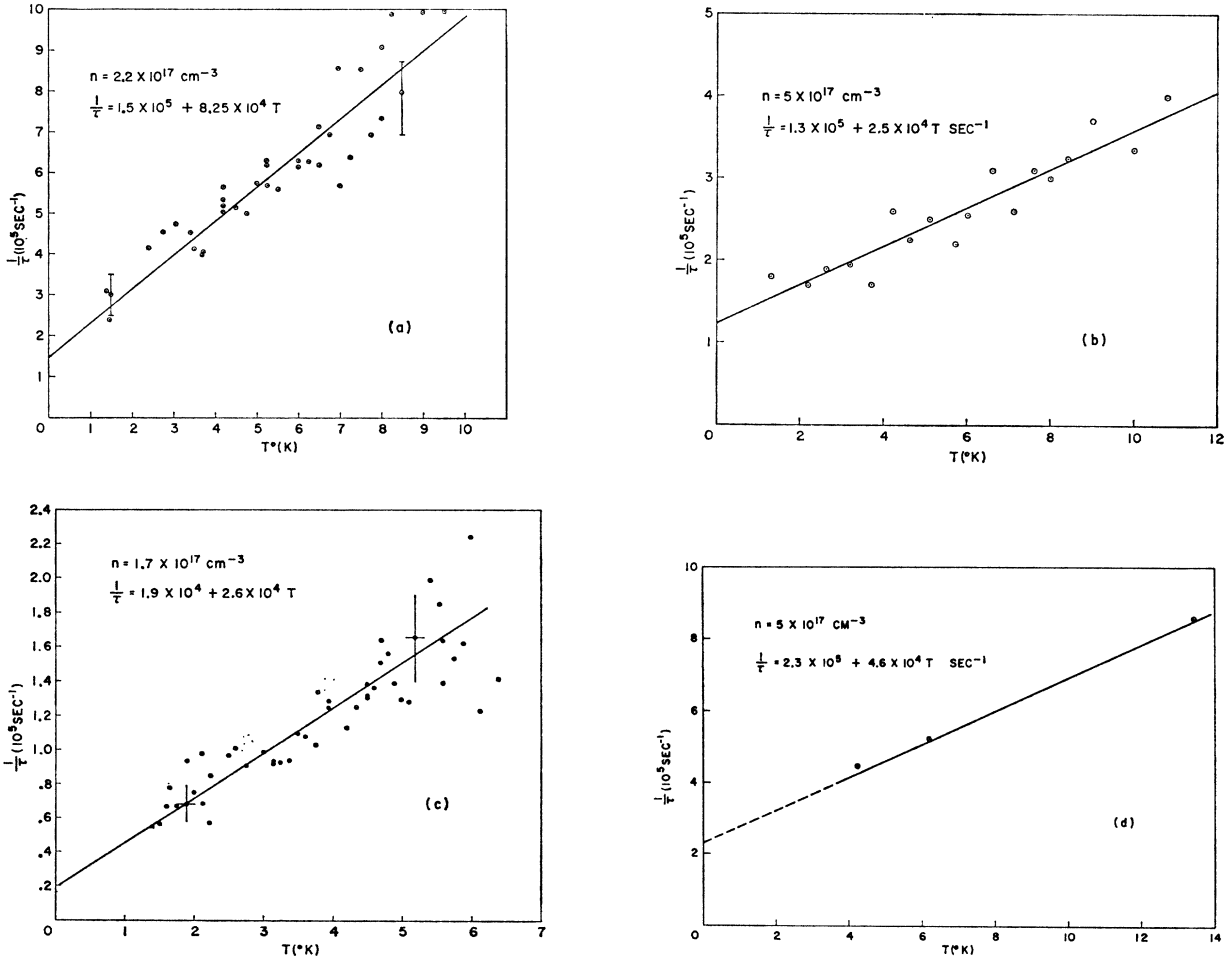

FIG. 6. The reorientation time $1/\tau$ as a function of temperature for four samples showing an exponential echo decay.

[23] M. D. Sturge, J. T. Krause, E. M. Gyorgy, R. C. LeCraw, and F. R. Merritt, Phys. Rev. 155, 218 (1967).

TABLE I. Results of spin-echo measurements on double nitrate samples.

Sample	Concentration (cm^{-3})	Deuterated or protonated	Decay mode	Decay parameters	Comments
1	2.2×10^{17}	deut.	Exponential	$1/\tau=1.5\times10^{5}+8.3\times10^{4}T$ sec^{-1}	Plotted in Fig. 6(a)
2	5.0×10^{17}	deut.	Lorentzian for $T\leq3.5$°K Exponential for $T\geq4.2$°K	$m(1.35°K)=6.8\times10^{10}$ sec^{-2} $m(3.48°K)=1.0\times10^{11}$ sec^{-2} $1/\tau=2.3\times10^{5}+4.6\times10^{4}T$ sec^{-1}	Plotted in Fig. 6(b)
3	1.7×10^{17}	deut.	Exponential	$1/\tau=1.9\times10^{4}+2.6\times10^{4}T$ sec^{-1}	Plotted in Fig. 6(c)
4	1.5×10^{17}	deut.	Lorentzian for $T\leq9.3$°K Exponential for $10.0<T\leq11.9$°K	$m(1.36°K)=4.15\times10^{10}$ sec^{-2} $m(9.3°K)=1.75\times10^{11}$ sec^{-2} $1/\tau(10°K)=5\times10^{5}$ sec^{-1}	
5	3×10^{18}	deut.	Gaussian for $T\leq4.2$°K Lorentzian for $4.6\leq T\leq10.2$°K	$k(1.34°K)=4.2\times10^{16}$ sec^{-3} $k(4.2°K)=6.3\times10^{16}$ sec^{-3} $m(4.6°K)=2.1\times10^{11}$ sec^{-2} $m(10.2°K)=3.2\times10^{11}$ sec^{-2}	
6	1.7×10^{17}	deut.	Lorentzian for $T\leq6.2$°K Exponential for $T\geq7.0$°K	$m(1.4°K)=4.15\times10^{10}$ sec^{-2} $m(6.2°K)=6.6\times10^{10}$ sec^{-2} $1/\tau=0.87\times10^{5}+4.5\times10^{4}T$ sec^{-1}	Possibly Lorentzian up to 9.3°K
7	5×10^{17}	deut.	Assumed exponential	$1/\tau=1.25\times10^{5}+2.5\times10^{4}$ sec^{-1}	Data obtained from photographs plotted in Fig. 6(d)
8	1×10^{18}	prot.	Assumed exponential	$1/\tau\approx10^{6}$ sec^{-1} for $1.4°K\leq T\leq6.0°K$	Data obtained from photographs studied up to 6°K only

Spin-Lattice Relaxation

Procedure

All except one set of measurements were made on deuterated samples since these gave better signal-to-noise ratios because of their smaller linewidth. The resonance signal was saturated by the high-power (~1 W) microwave pulse sufficiently long that the recovery of magnetization was independent of further pulse lengthening. The recovery of the signal was generally monitored by a low-power absorption measurement (usually $\sim10^{-6}$ W was sufficiently low for the recovery to be unaffected) whose time evolution was photographed from the oscilloscope, but some measurements were made using a two-pulse spin-echo sequence to sample the recovery of the magnetization. Except where specially noted, the results are for deuterated samples measured by the cw photographic technique. Above 20°K the increased receiver bandwidth and decreased signal amplitude combined to deteriorate the signal-to-noise ratio beyond the level for reliable measurement. Between about 150 and 250°K, we have inferred spin-lattice relaxation rates by measuring the linewidth ΔH and assuming that $1/T_1=(g\beta/\hbar)\Delta H$.

Results

Double nitrate. For temperatures up to about 8°K, the recoveries after a $\frac{1}{2}$-msec saturating pulse showed a nonexponential beginning followed by an exponential tail; this initial behavior was consistent with spectral diffusion times measured by a three-pulse-echo sequence. The exponential tail was taken to be the spin-lattice relaxation. For higher temperatures, the recovery was a simple exponential. Most measurements were made on the hyperfine lines of $g\approx g_{\parallel}$, once it had been verified that the relaxation rate was independent of the hyperfine component. The results of the magnetization recovery measurements are to be found in Fig. 7. For one sample at 4.2°K the variation of $1/T_1$ with orientation of the magnetic field was also measured and is plotted in Fig. 8. To see if the mass of the ligands affected the spin-lattice-relaxation rate, we measured T_1 for one nondeuterated (protonated) sample for $1.3<T<10$°K. These results are to be found in Fig. 7(a). The linewidth with $\mathbf{H}_0$ along $\langle100\rangle$ in the region from 135 to 250°K was measured and found to pass through a minimum at about 140°K before increasing to about 200 G at the higher temperature above which the signal became too weak to measure. The width, converted to rad sec^{-1} $\Delta\omega=(g\beta/\hbar)\Delta H$, is plotted in Fig. 9.

Bromate. The spin-lattice relaxation for the $Zn(BrO_3)_2\cdot6H_2O:Cu^{2+}$ was measured for two protonated samples having Cu^{2+} concentrations of 7×10^{17} and 3×10^{18} cm^{-3} with $\mathbf{H}_0$ along a principal axis where the spectra of the four inequivalent sites coincide.[4] The decay curves were simple exponentials and saturating pulse lengths of 20 μsec proved to be sufficient. The results are plotted in Fig. 10.

4. DISCUSSION

Spectrum of Double Nitrate

For zero strain and with the magnetic field along the [111] direction, one expects[11] and observes three

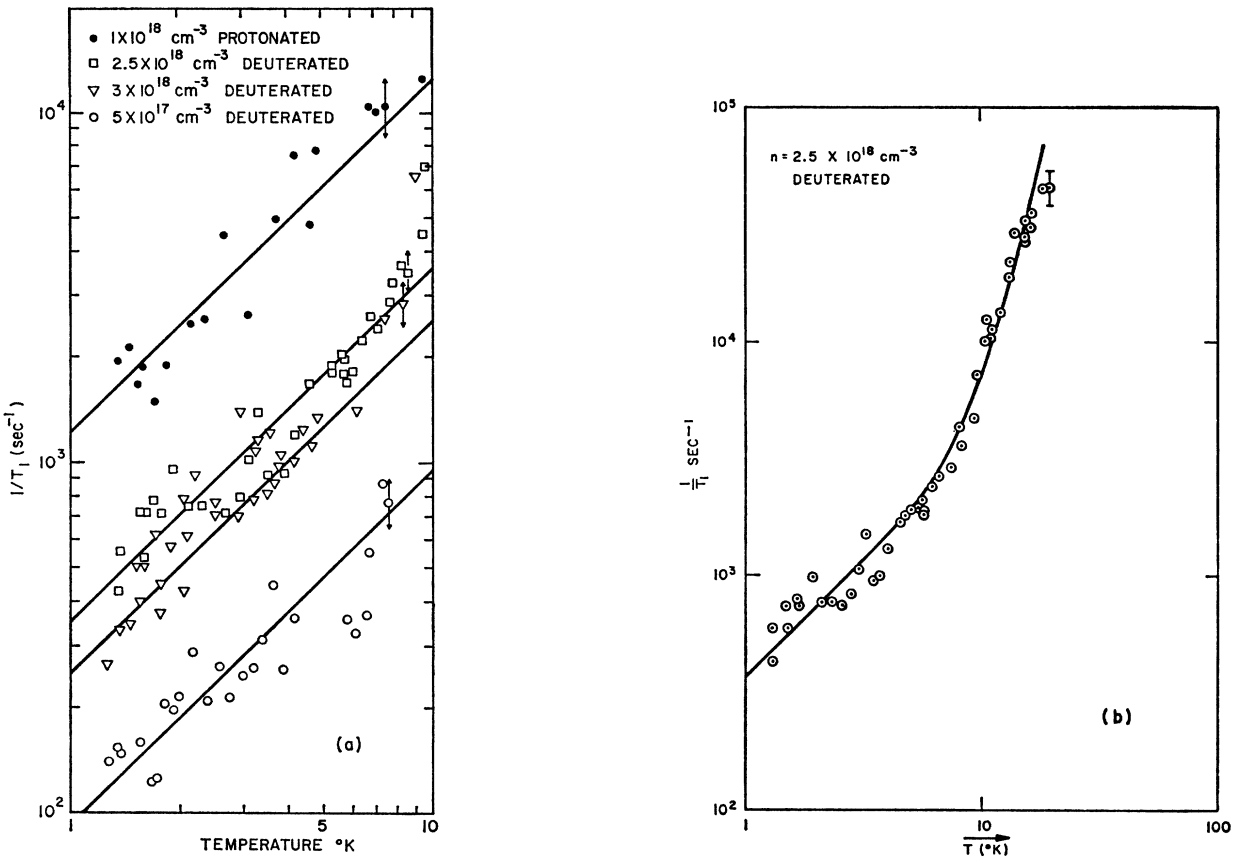

FIG. 7. (a) Spin-lattice-relaxation rates ($1/T_1$) as a function of temperature T for $1.3<T<10$°K for various concentrations of Cu^{2+} in $La_2Mg_3(NO_3)_{12}\cdot 24D_2O$ and for 10^{18} cm^{-3} Cu^{2+} in $La_2Mg_3(NO_3)_{12}\cdot 24H_2O$. Solid lines represent the best fits to a linear temperature dependence. (b) $1/T_1$ as a function of T for $1.3<T<20$°K for 25×10^{17} Cu^{2+} in $La_2Mg_3(NO_3)_{12}\cdot 24D_2O$. Solid line is $1/T_1 = 370T+0.033T^5$ sec^{-1}.

identical g values.[4] Away from the [111] direction, the situation can be quite complicated. To the approximation to be discussed below, the angular dependence of the g values in the absence of strain may be obtained conveniently by considering first the Zeeman interaction with Γ set equal to zero. In the $[|G_x\uparrow\rangle, |G_y\uparrow\rangle, |G_z\uparrow\rangle]$ representation (where $\uparrow$ stands for the spin quantum

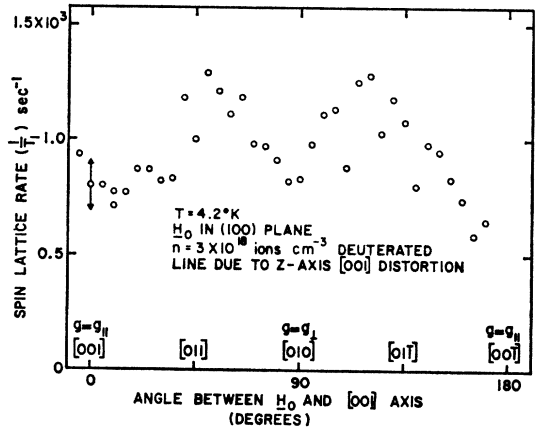

FIG. 8. Spin-lattice relaxation rate $1/T_1$ for double nitrate as a function of the orientation of the static magnetic field in the (100) plane at 4.2°K.

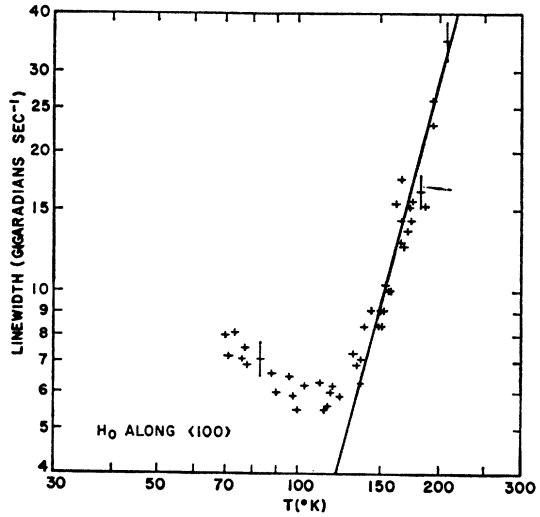

FIG. 9. Linewidth as a function of temperature for $100<T<250$°K. Solid line is $1/T_1 = 18T^4$ sec^{-1}. H_0 is along ⟨100⟩.

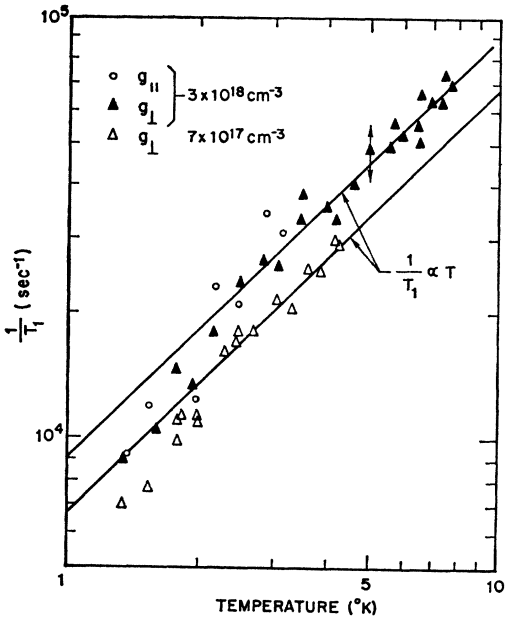

FIG. 10. Spin-lattice relaxation rate for the bromate as a function of temperature for $1.3<T<10$°K.

number $m_s=+\frac{1}{2}$) one has the following matrix when the magnetic field lies in the $(1\bar{1}0)$ plane:

$$[\mathcal{H}_{\text{Zee}}]=+\tfrac{1}{2}\beta H\begin{pmatrix} g_2 & 0 & 0 \\ 0 & g_2 & 0 \\ 0 & 0 & g_3 \end{pmatrix}. \tag{3}$$

The g values are given by

$$g_3=(g_{\parallel}^2\cos^2\theta+g_{\perp}^2\sin^2\theta)^{1/2}$$

and

$$g_2=[\tfrac{1}{2}g_{\parallel}^2(1-\cos^2\theta)+\tfrac{1}{2}g_{\perp}^2(1+\cos^2\theta)]^{1/2},$$

where θ is the angle between the [001] direction and the direction of the static field. Note that the S_z quantization axes for different distortions are all different for an arbitrary direction of the applied field. When the effects of a finite Γ are included, the energies for the $m_s=+\frac{1}{2}$ levels may be determined from the following matrix which is now written in the

$$[\tfrac{1}{2}\sqrt{2}(|G_x\uparrow\rangle-|G_y\uparrow\rangle),\tfrac{1}{2}\sqrt{2}(|G_x\uparrow\rangle+|G_y\uparrow\rangle),|G_z\uparrow\rangle]$$

representation:

$$\begin{pmatrix} \frac{1}{2}g_2\beta H-\Gamma & 0 & 0 \\ 0 & \frac{1}{2}g_2\beta H+\Gamma & -\sqrt{2}\Gamma \\ 0 & -\sqrt{2}\Gamma & \frac{1}{2}g_3\beta H \end{pmatrix}. \tag{4}$$

The magnetic field is assumed to be in the (110) plane and away from the [111] direction. A similar matrix for the $m_s=-\frac{1}{2}$ levels is obtained from the above by obvious modifications. The tunneling matrix elements involving a spin flip are neglected here, but this is a good approximation (see II) as long as $\Gamma\sin\beta_{23}\ll g\beta H$, where β_{23} is the angle between quantization axes $\lesssim(g_{\parallel}-g_{\perp})/g$, and $g\beta H$ is the separation between the $m_s=+\frac{1}{2}$ and $m_s=-\frac{1}{2}$ levels in the absence of tunneling. Note that the approximation referred to above involves neglecting off-diagonal terms of order ϵ in the above matrix. Since $(g_{\parallel}-g_{\perp})\beta H\epsilon\ll\Gamma$ always (see Fig. 3 of II), the approximation employed is, in fact, excellent.

One thus obtains one line at $g=g_2$ while the other transitions are determined by diagonalizing the 2×2 submatrix. For $|g_3-g_2|\beta H\gg\Gamma$, one obtains two transitions with g values $g_3\pm9\Gamma^2/(g_3-g_2)\beta^2H^2$. In the limit that $|g_3-g_2|\beta H\ll\Gamma$, there are four lines. Two have relative intensity $\frac{1}{9}$ and g values

$$\tfrac{1}{2}(g_3+g_2)\pm3\Gamma/\beta H\pm(g_3-g_2)^2\beta H/24\Gamma.$$

The other two lines, with relative intensity 8/9 are at $\frac{1}{6}(5g_3+g_2)$ and $\frac{1}{6}(g_3+5g_2)$. Keeping the magnetic field in the $(1\bar{1}0)$ plane, and rotating away from the [111] direction, it should be possible, therefore, to obtain some idea of the magnitude of Γ.

A careful study of the spectrum of the deuterated double nitrate very near the [111] direction failed to turn up any evidence for the behavior expected for the limit $|g_3-g_2|\beta H\ll\Gamma$. Since the angular dependence of the spectrum is adequately described throughout the $(1\bar{1}0)$ plane away from the [111] direction in terms of three static distortions, either the situation $|g_3-g_2|\beta H\gg\Gamma$ must obtain or the distortions are strain stabilized. One cannot decide in favor of one or the other on the basis of the angular variation of the spectrum alone. We believe, however, that strain stabilization is most probably dominant. The "ordinary" behavior of the spectrum 1° away from the [111] direction indicates that whatever be the stabilization mechanism, the stabilization energy is more than about 1.5×10^{-3} cm^{-1}.

The previous investigation[4] of this system had disclosed a doubling of the perpendicular spectrum with the magnetic field along the [001] direction. It appears now that this doubling arose from very slight misalignment. Since the quadrupole constant $P_{\parallel}$ and the hyperfine constant $A_{\perp}$ are comparable in magnitude, precise alignment is crucial when attempting to observe the perpendicular spectrum. A provision for accurate alignment was not available to the first investigators.[24]

Spin-Echo Behavior

Two-pulse echoes. The results for the double nitrate summarized in Table I indicate that with the exception of sample 5, all samples displayed, for higher temperatures at least, exponential decay. An exponential rate is expressed in terms of two parameters A and B such that $1/\tau=A+BT$. In samples 2, 4, and 6, Lorentzian decay at lower temperatures was followed by exponential decay at higher temperatures. Samples 1 and 3 displayed exponential decay throughout the range of temperatures studied while exponential decay was assumed for samples 7 and 8 since the data for

[24] B. Bleaney (private communication).

these were obtained from photographs on which we measured the time for the signal to fall to $1/e$ of its initial value.

The diffusion type of behavior observed for sample 5 results from the influence of nonresonant electron spins on a (resonant) electron spin contributing to the echo. Because of this behavior resulting from the large Cu^{2+} concentration, no direct information concerning the Jahn-Teller effect is obtained from the data for this sample, and it will be omitted from the discussion henceforth.[25]

A clue to the cause of the exponential decay is found in those samples which display a transition from a low-temperature Lorentzian diffusion behavior. The low-temperature results suggest a temperature-independent process wherein the deuteron spins mutually flip, causing the electron spin to diffuse in frequency. As the temperature is raised, the effects arising from the reorientation of the distortion are brought into play and we have the transition to the exponential decay behavior provided that the concentration is sufficiently low. In the following discussion, an attempt will be made to account for the range in values of the extracted parameters.

The first and most important point to note is that the extraction of data from the echo-decay plots is complicated by the pronounced nuclear modulation[19,21,22] of the decay trace. Since we lacked the means to mount each sample in the cavity in a reproducible fashion, and since we sought a static field orientation in each run which would yield the smoothest decay trace, the actual modulation pattern measured for each sample is, in fact, somewhat different. This, we believe, accounts for most of the variation in the measured coefficient of T in the expression for the exponential decay rate. Although it is difficult to measure an exponential decay envelope when the modulation is so pronounced, one has some evidence that the correct type of curve has been drawn since three of the samples actually do display a change in the decay envelope from that characteristic of Lorentzian diffusion to exponential as the temperature is increased. There is, of course, difficulty in identifying precisely the mode of decay in the transition between these two types of behavior. Furthermore, if the temperature dependence were merely due to Lorentzian diffusion one should expect a rate proportional to $T^{1/2}$ rather than linear in T as observed. This may be seen as follows. If Lorentzian decay traces were being incorrectly analyzed as decaying exponentially, i.e., measuring the time to decay to $1/e$ of the initial value, the analysis would yield $(\frac{1}{2}m)^{1/2}$ rather than τ. MNM show that $m \approx \Delta\omega/T_1$ when the magnetic moments causing the diffusion are ions of the same kind as those under study, and since $1/T_1 \propto T$ in the range of temperatures over which the spin-echo experiments were performed, $m^{1/2} \propto T^{1/2}$.

Further evidence for the validity of our analysis for the double nitrate is found in the two-pulse measurements for Cu^{2+} in the bromate and for Ni^{3+} in Al_2O_3. The early measurements[4] on the bromate system, which indicated a more rapid reorientation time than in the LMN, are consistent with our findings—which yield a value of about 1.5×10^{-6} sec at 4.2°K. For Ni^{3+} in Al_2O_3, the reorientation time has been measured by acoustic loss[23] and found to be (at $T=2$°K)

$$(1/\tau)_{\text{acoustic loss}} = 2\times10^{7}\ \text{sec}^{-1}.$$

Our failure to observe any echoes is consistent with the very short phase memory time expected.

Although we find quite a large range of values for B, the range of values obtained for A is even greater. Below, an attempt is made to account for some of this variation in A. A clue to the explanation is found in the comparison between two samples of similar concentrations, one deuterated and the other hydrated (samples 7 and 8). From the results in Table I, it is seen that the value for A is approximately eight times greater for the hydrated sample. If the decay is really Lorentzian but has been incorrectly analyzed as exponential (and the reader is reminded that this is probably the case since the data for both these samples were obtained from photographs and assumed to display exponential decay), the ratio of these A values should be

$$A_{\text{hyd}}/A_{\text{deut}} = (m_{\text{hyd}}/m_{\text{deut}})^{1/2}.$$

Now the parameter $m \propto \mu^3$, where μ is the magnetic moment, and we expect

$$A_{\text{hyd}}/A_{\text{deut}} = 5.8.$$

We believe that some variation among the nominally deuterated samples may be due, in fact, to incomplete deuteration. The results for sample 3, grown with the greatest care with respect to completeness of deuteration and showing the lowest value for A, are in fact consistent with this notion. This sample also shows the most pronounced nuclear-modulation effects of deuterons.

The nuclear environment will also have a slight effect on the parameter B. In the localized representation, using the harmonic-oscillator approximation, the wave functions are proportional to $e^{-\omega\theta^2}$ and

$$\omega_{\text{hyd}}/\omega_{\text{deut}} = (18/20)^{1/2}.$$

Thus the hydrated complex will have a greater overlap between these localized wave functions, implying a

[25] Note that two diffusion-type effects are expected in concentrated samples. The first is due to T_1 flips as discussed by MNM. The second results from changes in the local magnetic field at a resonant site accompanying the reorientation of nonresonant distortions. The ratio of the effectiveness of the second process as compared to the first will be $\Delta g/g$, where Δg is the difference in g values characterizing the distortions involved in the reorientation.

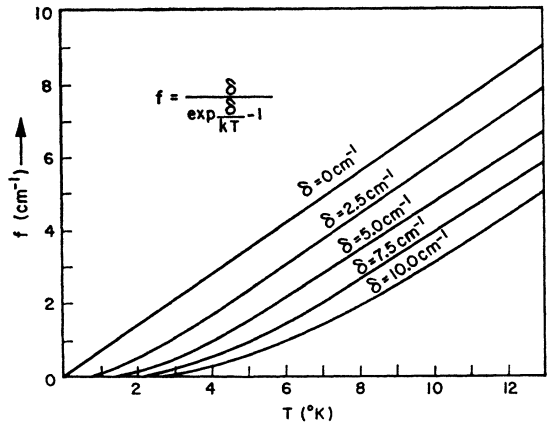

FIG. 11. Effects of strain on the reorientation rate $1/\tau$: the function $f(\delta,T)=\delta(\exp\delta/kT-1)^{-1}$ as a function of T with the random strain energy δ as a parameter.

larger value of Γ. A more refined calculation (see II) yields $\Gamma_{\text{hyd}}/\Gamma_{\text{deut}}=\sqrt{2}$.

As shown in II, the reorientation rate $1/\tau$ has a strain and temperature dependence which, for the direct process, is accurately given by

$$1/\tau \propto f(\delta,T)=\delta(\exp\delta/kT-1)^{-1}. \quad (5)$$

Here δ is a measure of the energy shift of the resonant distortion arising from random strains and the factor in parentheses is simply the phonon occupation number at δ for a temperature T. The function $f(\delta,T)$ is plotted in Fig. 11, where it is seen that for low values of δ, one obtains a reorientation rate linear in T. This is no longer true for larger values of δ. Such a dependence on the state of strain in the sample might also account for some of the observed variation in A.

Stimulated echoes. Where the two-pulse experiments exhibit Gaussian or Lorentzian decay one would expect that a check on the parameters m and k could be obtained from the stimulated-echo results. No agreement was found; the decay constants derived from the two-pulse echo decay was generally about 10 times larger than that derived from stimulated echo measurements. This lack of agreement presumably means that the model used by Klauder and Anderson and by MNM does not really apply in this case, where two different processes contribute to echo decay. However, one should still be able to estimate a diffusion constant from the decay of the three-pulse (stimulated) echo.

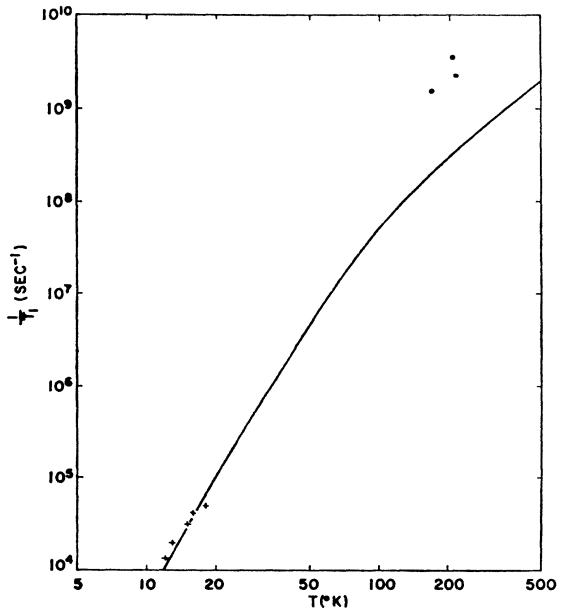

FIG. 12. Spin-lattice relaxation of Cu^{2+} $La_2Mg_3(NO_3)_{12}\cdot 24D_2O$. Experimental results of Fig. 7 and Fig. 9 on a single plot. The solid line represents

$$\frac{1}{T_1}=0.033T^5\int_0^{\Theta_D/T}\frac{x^4e^x}{(1-e^x)^2}dx\Big/\int_0^{\infty}\frac{x^4e^x}{(1-e^x)^2}dx \text{ sec}^{-1},$$

with $\Theta_D=300°$K.

Spin-Lattice Relaxation

Double nitrate. The nonexponentiality of some of the recovery curves is consistent with a model of spectral diffusion. This was confirmed for one sample (25×10^{18} ions cm^{-3}) by measurements of the diffusion constant from three-pulse spin-echo sequences.[19,20]

The concentration dependence of T_1 does not seem to be due to cross relaxation to another species. Chemical analysis confirms the purity of the crystals, but there is still the possibility that the observed copper site (1) [18] cross relaxes to the unobserved copper site (2). However, none of the rate-versus-temperature curves shows a plateau region which might indicate such an effect. If one tries to use a model like that of Rannestad and Wagner,[26] one concludes that either cross relaxation is negligible or that it is unreasonably fast; even this latter interpretation does not explain a concentration dependence unless the ratio of copper ions in site (2) to those in site (1) is concentration-dependent or that the spin-lattice-relaxation rate for one or both sites is concentration-dependent anyway. A more likely explanation would appear to be one along the lines suggested by Kochelaev,[27] though his analysis assumes that the impurities (or defects) are harmonically bound, whereas if they are the Jahn-Teller centers themselves the problem is less simple; it seems plausible, however, that the perturbation of the phonons is greater in such a case.

There appears to be no phonon bottlenecking in our range of concentration and temperature; the relaxation rate decreases with decreasing concentration, there is no sign of a T^2 temperature dependence, and allowing liquid He into the cavity to improve the acoustical match at the crystal boundaries did not change the relaxation behavior. (See note added in proof.)

[26] A. Rannestad and P. E. Wagner, Phys. Rev. **131**, 1953 (1963).
[27] B. I. Kochelaev, Dokl. Akad. Nauk SSSR **5**, 1053 (1960) [English transl.: Soviet Phys.—Doklady **5**, 349 (1960)].

TABLE II. Representation of curves of Figs. 7 and 9 by analytical expressions for $1/T_1$.

	Analytical rep. ($\sec^{-1}$; T in °K)	Type of meas.	Temp. range (°K)	(10^{17} cm^{-3})	Fig.
(1)	$3.5\times10^{2}T^{3}$	linewidth	150–235	30 deut.	9
(2)	$3.7\times10^{2}T+3.3\times10^{-2}T^{5}$	pulse sat.	1.3–20	25 deut.	7(b)
(3)	$2.5\times10^{2}T$	pulse sat.	1.3–10	30 deut.	7(a)
(4)	$0.94\times10^{2}T$	pulse sat.	1.3–10	5 deut.	7(a)
(5)	$13\times10^{2}T$	pulse sat.	1.3–10	10 prot.	7(a)

In Table II we represent the curves of Figs. 7 and 9 by the analytical expressions for $1/T_1$ in $\sec^{-1}$. The rates obtained by linewidth analysis (1) appear to be an extrapolation of the T^5 law of (2) modified by the approach to the Debye temperature of the lattice. For if one joins results (1) to (2) on a log-log plot (see Fig. 12) the power law is $T^{4.5}$. The integral which gives the T^5 law at $T\ll\Theta_D$ is

$$T^5\int_0^{\Theta_D/T}\frac{x^4e^x}{(1-e^x)^2}dx,$$

where Θ_D is the Debye temperature. We have plotted this for $\Theta_D=300$°K in Fig. 12. A word concerning this choice for Θ_D is in order. Bailey[28] interprets his specific-heat data on the basis that the chemical formula cell introduces the large discontinuity in the phonon dispersion to distinguish acoustical from optical modes. He so deduces that $\Theta_D\approx61.5$°K. For our purposes, however, it seems more reasonable to assume that there is no serious discontinuity until the phonon wavelength (considering the solid as a continuum for a moment) becomes of the order of a nearest-neighbor distance. Such reasoning suggests that the effective Debye temperature is

$$61.5\times(\text{number of atoms in chemical formula})^{1/3}\approx300\text{°K}$$

used in the Debye integral above. The results (2) for $10<T<20$°K also fit an exponential temperature law $1/T_1=4\times10^{5}e^{-38\text{°K}/T}$ $\sec^{-1}$, but in view of the extrapolation to the linewidth results, we have rejected this description.

Motivated by the work of Höchli and Müller,[29] we tried to fit the linewidth measurements to an Orbach-type expression and found an equally good fit to

$$\frac{1}{T_1}=4.6\times10^{10}e^{-540\text{°K}/T}\ \sec^{-1}$$

for

$$150<T<250\text{°K},$$

but again in view of the good correlation with the low-temperature results mentioned above, we believe that this is probably not significant.

We see from Table II [items (1) and (5)] that, for similar concentration, the Cu^{2+} spin-lattice-relaxation rate is a factor of about 3 faster in the protonated than in the deuterated double nitrate. In view of the concentration dependence, the figure should not be taken too literally, but, since (1) is more concentrated than (5), there would seem to be little doubt that deuteration retards the relaxation rate.

The scatter on the plot of spin-lattice-relaxation rate versus angle between H_0 and the [001] direction in the (100) plane in Fig. 8 does not justify trying to fit it to a curve, but it is sufficiently definite to say that the minimum rate lies in the [001] direction and the maximum rate somewhere around the [011] direction; the variation is at most a factor of 2 between the two extremes.

Bromate. The $1/T_1$ for the $Zn(BrO_3)_2\cdot6D_2O:Cu^{2+}$ may be approximated analytically as indicated in Table III.

The results for $T<2.2$°K fall below the linear extrapolation, which might suggest a phonon bottleneck were it not for the fact that both samples start to deviate at the same temperature despite the factor of 5 difference in concentration. We shall see that this can be interpreted on the model proposed in II as reflecting the magnitude of the average random static strain splitting between the vibronic states.

5. CONCLUSIONS

The full conclusions concerning the results of these experiments must await the development of the model discussed in II. Our purpose here is to summarize the results which the model to be presented in II will have to account for.

At low temperatures, the water octahedron surrounding the Cu^{2+} ion is frozen into one of three equivalent tetragonal distortions. At any given site one of these distortions is energetically preferable, most probably as a result of local random strains. The EPR spectrum for

TABLE III. Representation of curves of Fig. 10 by analytical expressions for $1/T$.

Analytical rep. (T_1 in sec, T in °K)	Type of meas.	Temp. range (°K)	Concentration (cm^{-3})	Fig.
$1/T_1=7\ \times10^{3}T$	pulse sat.	2.2–4.2	7×10^{17}	10
$1/T_1=9.5\times10^{3}T$	pulse sat.	2.2–9	30×10^{17}	10

[28] C. A. Bailey, Proc. Phys. Soc. (London) **83**, 369 (1964).
[29] U. T. Höchli and K. A. Müller, Phys. Rev. Letters **12**, 730 (1964).

only one of the two possible Cu^{2+} sites is observed, and indicates that each distortion is described at low temperatures by an axial spin Hamiltonian. For the double nitrate, $g_{\parallel}=2.465\pm0.001$ and $g_{\perp}=2.099\pm0.001$. The results are consistent with the notion that phonons induce reorientation among the distortions. For Cu^{2+} concentrations up to about 5×10^{17} cm^{-3} this reorientation rate is linear in temperature with an average proportionality constant $B=5\times10^{4}$ sec^{-1} deg^{-1} for the deuterated double nitrate. There is some evidence that B is isotope-dependent, being larger for a protonated sample.

The spin-lattice-relaxation rate for the deuterated double nitrate samples having a concentration similar to that given above may be fitted by the expression $1/T_1=\alpha T+\beta T^5$, where $\alpha\simeq100$ sec^{-1} deg^{-1} and $\beta=3.3\times10^{-2}$ sec^{-1} deg^{-5}. The most interesting feature here is that the rate is some 4 orders of magnitude faster than the observed for Cu^{2+} in static octahedral water coordination in the Tutton salt studied by Gill,[14] but there is no evidence for a phonon bottleneck. An important point to note is that $1/T_1\propto1/\tau$ over the range that they have both been measured. A study of the angular dependence for the double nitrate $1/T_1$ in the (100) plane indicates that the rate is a minimum when the static magnetic field is oriented along one of the distortion axes and peaks when the magnetic field makes equal angles with a pair of distortion axes.

The results for the bromate, while not as extensive as those for the double nitrate, are qualitatively similar.

The technique which we have introduced for the measurement of reorientation times should prove to be a useful complement to the already existing methods. These include observation of motional narrowing, acoustic loss,[23] and the observation of the change in magnitude of an EPR signal as stress is applied or removed.[30] Our method will be difficult to apply, of course, whenever one encounters severe echo modulation.

Note added in proof. The absence of bottlenecking seems to be at variance with the results of K. P. Lee and D. Walsh [Phys. Letters **27A**, 17 (1968)] on the bromate system, possibly due to their having more strain-free crystals. The effect of strain on T_1 behavior is discussed in Sec. II.

ACKNOWLEDGMENTS

We should like to acknowledge many discussions with Professor B. Bleaney, Mary C. M. O'Brien, and G. D. Watkins. E. R. Davies and H. F. MacDonald kindly made available their EPR spectrometers for some of the measurements. The chemical analyses were handled by R. G. Bessent of the Atomic Energy Research Establishment, Harwell, England, J. A. James of the Associated Electrical Industries, Ltd., (A.E.I.) Rugby, and T. Y. Komatani of Bell Telephone Laboratories. Special thanks go to J. W. Leight of the Carlyle Barton Laboratory of Johns Hopkins University for growing a sample of double nitrate, to M. D. Sturge for supplying the crystal of $Al_2O_3:Ni^{3+}$, and to E. J. Jenkison of the Clarendon Laboratory for his expert help in designing the cavity and associated components. D. C. Krupka thanks Professor B. Bleaney for making available the facilities of the Clarendon Laboratory where D. C. Krupka held a National Research Council of Canada Overseas Postdoctorate Fellowship. This work was carried out while F. I. B. Williams held an A.I.E. Fellowship. The support of the Department of Scientific and Industrial Research and the Science Research Council in the form of an equipment grant is also gratefully acknowledged.

[30] W. Känzig, J. Phys. Chem. Solids **23**, 479 (1962).

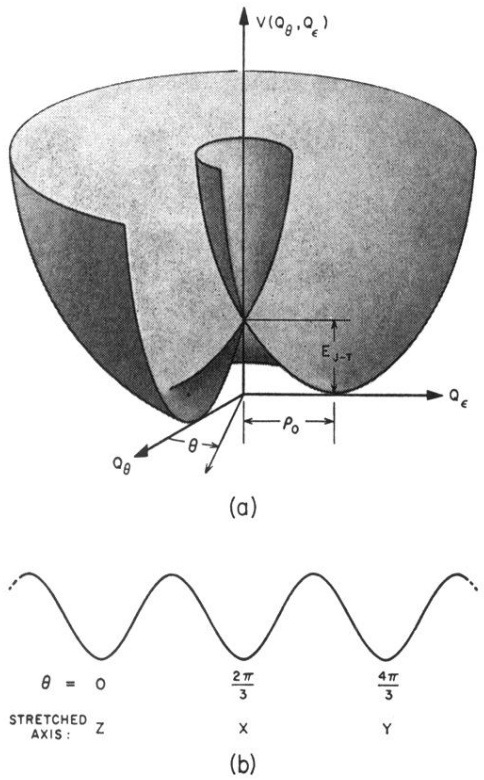

FIG. 2. (a) The Mexican-hat potential for linear coupling. The vectors $\theta=0$, $\theta=\frac{2}{3}\pi$, and $\theta=\frac{4}{3}\pi$ correspond to configurations of the octahedron stretched along its z, x, and y axes, respectively. (b) Section through trough at $\rho=\rho_0$ folded flat, showing the effects of nonlinearities in coupling and of "elastic" anharmonicity.